

or alternatively,

$$Z_{12} = \frac{\begin{vmatrix} (\hat{I}_0, \hat{J}_0) & (\hat{I}_0, \hat{J}_1) & \cdots & (\hat{I}_0, \hat{J}_N) \\ (\hat{I}_1, \hat{J}_0) & (\hat{I}_1, \hat{J}_1) & \cdots & (\hat{I}_1, \hat{J}_N) \\ \cdots & \cdots & \cdots & \cdots \\ (\hat{I}_N, \hat{J}_0) & (\hat{I}_N, \hat{J}_1) & \cdots & (\hat{I}_N, \hat{J}_N) \end{vmatrix}}{\begin{vmatrix} (\hat{I}_1, \hat{J}_1) & \cdots & (\hat{I}_1, \hat{J}_N) \\ \cdots & \cdots & \cdots \\ (\hat{I}_N, \hat{J}_1) & \cdots & (\hat{I}_N, \hat{J}_N) \end{vmatrix}}, \quad (75)$$

where the scalar products (\hat{I}_m, \hat{J}_n) are as defined by (69). Formulas for Z_{11} are (74) and (75) with all \hat{I}_n 's replaced by the corresponding \hat{J}_n 's. Formulas for Z_{22} are (74) and (75) with all \hat{J}_n 's replaced by the corresponding \hat{I}_n 's.

To illustrate the difficulty that occurs if J_{ij} does not have the same number of variational parameters as J_{ij} , suppose

$$\begin{aligned} J_{11} &= \hat{J}_0 & J_{12} &= a_1 \hat{J}_1, \\ J_{22} &= \hat{I}_0 & J_{21} &= b_1 \hat{I}_1. \end{aligned} \quad (76)$$

[This choice was purposely excluded by (71).] The mutual impedance (74) or (75) then becomes

$$Z_{12} = (\hat{I}_0, \hat{J}_1) - \frac{(\hat{I}_0, \hat{J}_1)(\hat{I}_1, \hat{J}_0)}{(\hat{I}_1, \hat{J}_1)}. \quad (77)$$

As the two objects are separated

$$(\hat{I}_0, \hat{J}_0) \rightarrow 0 \quad (\hat{I}_1, \hat{J}_1) \rightarrow 0, \quad (78)$$

because these products involve currents on different objects, and

$$(\hat{I}_0, \hat{J}_1) \rightarrow C_{01} \quad (\hat{I}_1, \hat{J}_0) \rightarrow C_{10} \quad (79)$$

(C 's denote constants) because they involve currents on the same object. Hence, as the two objects are separated, by (77) one has $Z_{12} \rightarrow \infty$, an impossibility. This absurd result can be explained by noting that

$$a_1 = -\frac{(\hat{I}_1, \hat{J}_0)}{(\hat{I}_1, \hat{J}_1)} \rightarrow \infty \quad (80)$$

in the variational solution, and, hence, no value of a_1 can improve the solution. The parameter b_1 behaves similarly. One can view this as a poor choice of trial functions. However, if J_{12} is chosen to have the same number of variational parameters as J_{22} , and similarly for J_{12} and J_{11} , as required by (71), then the difficulty does not arise. To show this, note that, as the objects are separated, the denominator of (75) becomes of the form

$$\begin{vmatrix} \text{constants} & 0's \\ \hline \hline 0's & \text{constants} \end{vmatrix} \quad (81)$$

which is finite. If J_{ij} does not have the same number of variational parameters as J_{jj} , then one or more rows or columns of zeros appear in the "constants" sections of (81), and the denominator of (75) vanishes as the objects are separated. Of course, no such difficulty arises in the calculation of Z_{11} and Z_{22} .

Wide-Band Matching of Lossless Waveguide Two-Ports*

DARKO KAJFEŽ†

Summary—A new procedure of matching is presented, based in the equations which transform the output reflection coefficient of a lossless two-port network into the input reflection coefficient. The parameters of the equations are the residual reflection coefficients which can be easily measured. The optimum reflection coefficients which have the minimum frequency variation are computed for the specific case when the frequency variation of the residual reflection coefficients can be approximated by a circular arc in the Smith diagram. An illustrative example is given to explain the determination of the position and the size of the inductive obstacles that match a waveguide two-port structure within a wide frequency band.

* Received by the PGM TT, October 17, 1961; revised manuscript received, January 2, 1962.

† Institute for Automation, Ljubljana, Yugoslavia.

I. INTRODUCTION

HERE ARE a considerable number of waveguide structures that can be represented by an equivalent two-port network. Waveguide bends, rotary joints, coaxial-to-waveguide transducers and many other waveguide components are typical examples of lossless two-port waveguide structures. Frequently these components are not completely matched and, in spite of careful design, they produce a discontinuity in the waveguide system. The aim of this article is to present a method that will make it possible to match the residual reflections of a two-port wave-

guide structure, not only at a single frequency but also within a given frequency band.

Methods are treated in the literature only for wideband matching of microwave one-ports.¹ Their procedure of matching is based on measured values of impedance, plotted on a rectangular or on a Smith diagram. To the author's knowledge an analogous method for two-ports does not exist.

II. DISCUSSION

A. Transformation of the Reflection Coefficient through a Two-Port Network

At lower frequencies, a two-port network is treated as an impedance transformer.² In the microwave frequency region, however, the idea of impedance loses much of its original significance. We shall therefore devote our attention to the reflection coefficient, which is a basic concept in transmission line theory.

Accordingly, we shall be primarily interested in the output-input transformation of the reflection coefficient, without using impedance or admittance.^{3,4} It can be shown that the load reflection coefficient g_r will be transformed into an input reflection coefficient g_1 [Fig. 1(a)] expressed by

$$g_1 = \frac{g_{10}}{\bar{g}_{20}} \cdot \frac{g_r - \bar{g}_{20}}{g_r g_{20} - 1}. \quad (1)$$

The term g_{10} is the residual input reflection coefficient which we can measure at the waveguide input when the output is terminated reflectionless ($g_r = 0$). Similarly, g_{20} signifies the residual output reflection coefficient which can be measured at the waveguide output when the input is terminated reflectionless ($g_s = 0$). Corresponding complex-conjugated values are denoted by \bar{g}_{10} and \bar{g}_{20} . When the load g_s at the input is given and we wish to know the reflection coefficient g_2 at the output [Fig. 1(b)], the transformation reads

$$g_2 = \frac{g_{20}}{\bar{g}_{10}} \cdot \frac{g_s - \bar{g}_{10}}{g_s g_{10} - 1}. \quad (2)$$

The behavior of the two-port lossless network is, therefore, completely determined by the measured values of two complex reflection coefficients (g_{10} and g_{20}), despite the fact that we know nothing about the components that constitute the interior of the structure. Moreover, both measurements of complex quantities are not in fact strictly necessary, for g_{10} being known, the modulus

¹ J. A. Nelson and G. Stavis, "Impedance matching, Transformers and Baluns" in "Very High Frequency Techniques," McGraw-Hill Book Co., Inc., New York, N. Y., vol. I, pp. 53-92, 1947.

² L. Gyergyek, "The four-terminal networks and the linear transformations," *Elec. Rev. (Yugosl.)*, vol. 22, pp. 287-293; September-October, 1954.

³ H. V. Shurmer, "Transformation of the Smith chart through lossless junctions," *Proc. IEE*, vol. 105, pt C, pp. 177-182; March, 1958.

⁴ J. R. G. Twisleton, "The transformation of admittance through a matching section and lossless waveguide junction," *Proc. IEE*, vol. 106, pt. B, pp. 175-179; March, 1959.

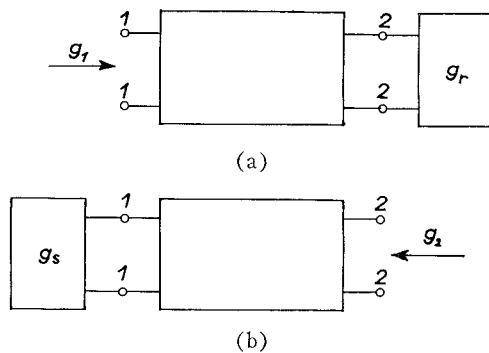


Fig. 1—The transformation of reflection coefficients through a two-port. (a) $g_1 = g_1(g_r)$. (b) $g_2 = g_2(g_s)$.

of g_{20} is determined too, because for all lossless two-ports the equation holds:

$$|g_{10}| = |g_{20}|.$$

B. Frequency Independent Transformation

Although (1) and (2) are valid for general lossless two-port structures, we want now to introduce some simplifications that will contribute considerably to the clarity and simplicity of the following discussion. We have, assuming the case of relatively small reflections,

$$|g_r g_{20}| \ll 1 \text{ and } |g_s g_{10}| \ll 1.$$

This leads to the simplification of (1) and (2):

$$g_1 = g_{10} - \frac{g_{10}}{\bar{g}_{20}} g_r \quad (3)$$

$$g_2 = g_{20} - \frac{g_{20}}{\bar{g}_{10}} g_s. \quad (4)$$

Let us now investigate the behavior of the transformation in the given frequency band. Every two-port network has its specific behavior of frequency response of the residual reflection coefficients, which could be checked by measurement. One possible example of the measured values (thick curve) is shown in Fig. 2. This figure and many other similar plots lead to the conclusion that the reflection coefficient response can be represented approximately by the arc of a circle (thin curve on Fig. 2), the center of which is shifted to the point R_{10} :

$$g_{10} = R_{10} + r_{10} e^{j\rho_1(f-f_0)}, \quad (5)$$

where f_0 denotes the center frequency of the frequency band. The frequency response of g_{20} can be correspondingly, in most cases, approximated by the expression

$$g_{20} = R_{20} + r_{20} e^{j\rho_2(f-f_0)}. \quad (6)$$

Real quantities ρ_1 and ρ_2 are expressed in arc degrees per Mc and determine the rate at which the point is circulating around the diagram when the frequency f is changing.

Let us now consider the transformation (3) and require the transformation to be frequency independent.

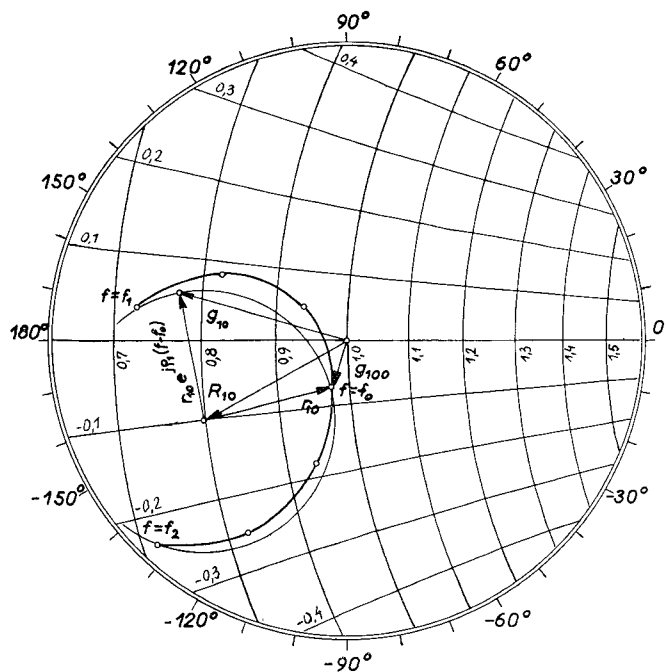


Fig. 2—Typical plot of input reflection coefficient (thick curve), which can be approximated with a circle arc (thin curve).

We choose a constant load reflection coefficient g_{rk} to transform it into one constant value of frequency independent input reflection coefficient g_{1k} . We require that

$$\left(\frac{dg_1}{df} \right)_{f=f_0} = 0. \quad (7)$$

Using the rule for derivation of indirect functions, we obtain (8) from (3), and (5)–(7):

$$g_{rk} = \frac{\bar{g}_{200}}{1 + \frac{g_{100}\rho_2\bar{r}_{20}}{\bar{g}_{200}\rho_1\bar{r}_{10}}}, \quad (8)$$

where g_{100} and g_{200} denote the residual reflection coefficients at the center frequency (see Fig. 2). Then we have

$$g_{100} = (g_{10})_{f=f_0} = R_{10} + r_{10} \quad (9)$$

$$g_{200} = (g_{20})_{f=f_0} = R_{20} + r_{20}. \quad (10)$$

From (3) we find that the load reflection coefficient g_{rk} will be transformed in the input reflection coefficient g_{1k} :

$$g_{1k} = \frac{g_{100}}{1 + \frac{g_{100}\rho_1\bar{r}_{10}}{g_{100}\rho_2\bar{r}_{20}}}. \quad (11)$$

After having terminated the output terminals in a load, then the two-port network will transform the load reflection coefficient g_{rk} into the vicinity of one point g_{1k} only, almost independent of frequency. Thus the transformation is frequency independent, although the measurements of g_{10} and g_{20} have shown that the

parameters of the two-port network vary with frequency.

Matching of the two-port network will be attained if we terminate its input in a circuit having the reflection coefficient g_{sk} that is equal to the conjugate value of the reflection coefficient g_{1k} . The matching condition therefore is

$$g_{sk} = \bar{g}_{1k}, \quad (12)$$

where g_{sk} designates the reflection coefficient of the input circuit required for frequency independent matching of the two-port network which is loaded with g_{rk} . We shall call g_{rk} and g_{sk} the optimum reflection coefficients. In order to match the two-port network in an almost frequency independent manner, the input and output circuits should have the following reflection coefficients:

$$g_{rk} = \frac{\bar{g}_{200}}{1 + \frac{g_{100}\rho_2\bar{r}_{20}}{\bar{g}_{200}\rho_1\bar{r}_{10}}} \quad (13)$$

and

$$g_{sk} = \frac{\bar{g}_{100}}{1 + \frac{g_{200}\rho_1\bar{r}_{10}}{\bar{g}_{100}\rho_2\bar{r}_{20}}}. \quad (14)$$

C. Example of Frequency Independent Transformation

Assume we have the two-port network shown in Fig. 3. Let the waveguide have constant dimensions (RG-48/U) throughout its length. Let the lengths θ_{x1} and θ_{x2} corresponding to the center frequency (3000 Mc) be 150° and 40° , respectively. The normalized susceptances $j0.2$ and $-j0.3$ are assumed to be frequency independent. We shall investigate the two-port network properties over the frequency band 2800–3200 Mc.

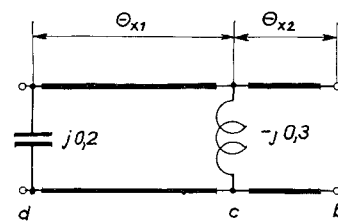


Fig. 3—Example of a two-port.

We shall now compute the residual reflection coefficients g_{10} and g_{20} , which could be obtained from measurements of network on Fig. 3. The results are shown in Fig. 4. At the center frequency we read the values of the residual reflection coefficients as

$$g_{100} = 0.137e^{j8^\circ} \quad \text{and} \quad g_{200} = 0.137e^{j159^\circ}.$$

As we see, we can replace this reflection coefficient plot well by the circle arcs. At the center frequency, the

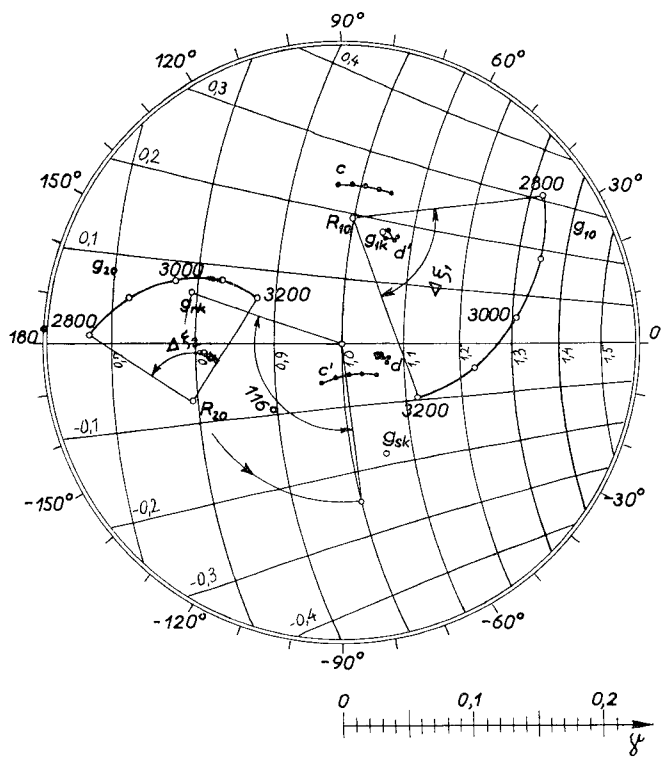


Fig. 4—The residual reflection coefficients g_{10} and g_{20} for the two-port from Fig. 3. It also shows the transformation of g_{rk} into g_{10} , which does not vary with frequency.

complex radii r_{10} and r_{20} are found to have these values:

$$r_{10} = 0.148e^{-j32^\circ} \quad \text{and} \quad r_{20} = 0.095e^{j98^\circ}.$$

By dividing the angle differences (designated in Fig. 4 as $\Delta\xi_1$ and $\Delta\xi_2$), by the frequency difference, the rates of rotation are found to be

$$\begin{aligned} \rho_1 &= \frac{\Delta\xi_1}{3200 - 2800} = -\frac{76}{400} = -0.190^\circ/\text{Mc} \\ \rho_2 &= \frac{\Delta\xi_2}{3200 - 2800} = -\frac{88}{400} = -0.220^\circ/\text{Mc}. \end{aligned}$$

Input and output optimum reflection coefficients are obtained from (13) and (14):

$$g_{sk} = 0.0904e^{-j69^\circ}, \quad g_{rk} = 0.122e^{j161^\circ}.$$

We next check on the Smith chart to see whether the transformation is frequency independent. The procedure of transformation is shown in Fig. 4. The load reflection coefficient is transformed along the length θ_{x2} into the point c in such a way that g_{rk} is rotated clockwise by the angle $2\theta_{x2}$, which depends on frequency. Afterwards the susceptance $-j0.3$ is added and the reflection coefficient response denoted by c' is obtained. After the new $2\theta_{x1}$ degrees rotation we get the reflection coefficient at point d . Addition of the susceptance $j0.2$ leads finally to the point d' representing the input reflection coefficient. At the center frequency the input reflection coefficient is equal to the computed value

$g_{10} = \bar{g}_{sk}$, and it differs negligibly from this value at other frequencies. As we see, the transformation is almost completely frequency independent.

D. Example of Wide-Band Matching Procedure

It is not possible, however, to terminate the waveguide two-ports with optimum reflection coefficients chosen anywhere on the Smith chart. The two-port network is usually terminated in a matched waveguide (its reflection coefficient is zero) to which we connect in parallel an inductive iris. The width of the iris aperture controls the magnitude of the parallel susceptance, which we suppose here to be independent of frequency. Consequently, only those values of the optimum reflection coefficients are available, whose corresponding points lie on the $R=1$ circle of the Smith chart. We have therefore to extend the two-port network by an additional length θ_1 and θ_2 of the waveguide, as shown in Fig. 5. As a result of this extension, the reflection coefficients g_{10} and g_{20} fall on the $R=1$ circle of the Smith chart. The matching irises are then placed there.

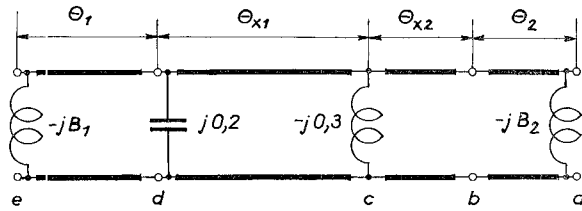


Fig. 5—Addition of the inductive susceptances in order to match the two-port from Fig. 3.

According to Fig. 4, g_{rk} will reach the negative $R=1$ circle provided that the output terminals are shifted by $2\theta_2 = 116^\circ$. Similarly, the input terminals should be shifted by $2\theta_1 = 344^\circ$. The shift of the input and output terminals results in the rotation of the residual reflection coefficients g_{10} and g_{20} . If this rotation were frequency independent, this procedure would be easy. Unfortunately, the rotation increases with increased frequency. The length $2\theta_1$, corresponding to the frequency 2800 Mc, is shorter by 44° than the value at the center frequency, and at the frequency 3200 Mc it is longer by the same amount. The g_{10} plot is therefore somewhat lengthened, as shown in Fig. 6. The mean rotation $2\theta_1$ was not shown in order to get a clearer picture. The mean rotation is the same for all points:

$$\begin{aligned} g_{100}' &= g_{100}e^{-j2\theta_1} = 0.137e^{-j336^\circ} \\ g_{200}' &= g_{200}e^{-j2\theta_2} = 0.137e^{j43^\circ}. \end{aligned}$$

Let us now find the new centers of curvature denoted by R_{10}' and R_{20}' . Following the same procedure, we read the new circle radii and the rates of rotation. By using (13) and (14), we can evaluate the corrected optimum reflection coefficients,

$$g_{rk}' = 0.109e^{-j65^\circ} \quad \text{and} \quad g_{sk}' = 0.0548e^{-j73^\circ},$$

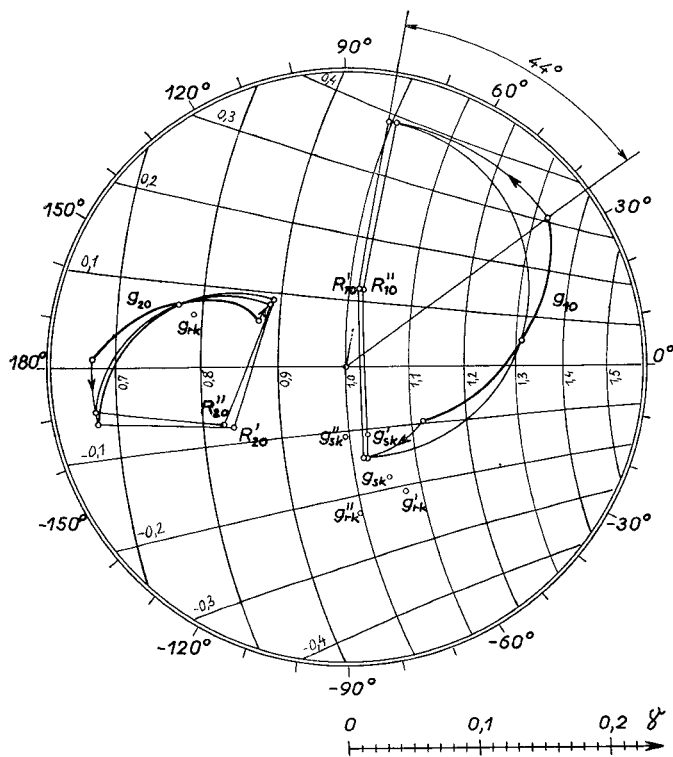


Fig. 6—Calculation of optimum reflection coefficients g_{sk} and g_{rk} .

where g_{rk}' and g_{sk}' have now approached the $R=1$ circle. We have to correct the values of $2\theta_1$ and $2\theta_2$ and to repeat the whole procedure. By this trial and error method we finally obtain

$$g_{rk}''' = 0.114e^{-i84^\circ}, \quad g_{sk}''' = 0.053e^{-i91^\circ} \\ 2\theta_1''' = 334^\circ, \quad 2\theta_2''' = 97^\circ.$$

The susceptance values of the irises can be read on the Smith chart as

$$B_1 = 0.11 \quad \text{and} \quad B_2 = 0.23.$$

Having determined the position and size of the inductive irises that lead to the frequency independent matching of the given two-port network, our problem is solved.

To check the frequency behavior of matching over the frequency band of 2800 to 3200 Mc, we shall compute the input impedance using the Smith chart in Fig. 7. We shall begin from the output side, where the reflection coefficient g_{rk}'' is connected at the point a . Rotation $2(\theta_2 + \theta_{x2})$ degrees gives the reflection coefficient at point c . Adding the parallel susceptance $-j0.3$ we then get the reflection coefficient denoted by c' . Rotation of $2\theta_{x1}$ gives the curve d , and addition of the susceptance $j0.2$ leads later to the curve d' . After $2\theta_1$ rotation we get the curve e , to which we add the susceptance $-jB_1 = -j0.11$ in parallel. So, a quite well matched input has been achieved (reflection coefficient

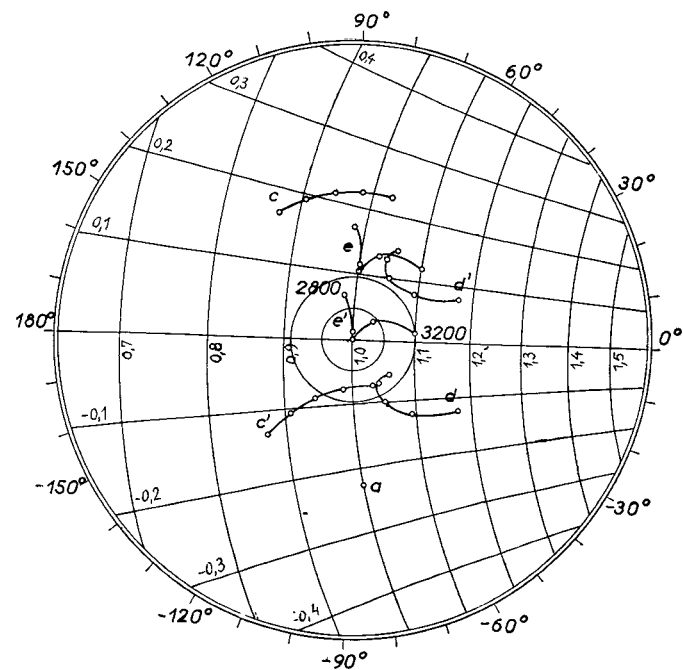


Fig. 7—Transformation of the load reflection coefficient a (inductive obstacle added) into an input reflection coefficient e' . Compare the matched reflection coefficient e' with the unmatched g_{10} from Fig. 4.

e'). Within the 2900-3200 Mc band the VSWR is less than 1.05 and within the 2800 to 3200 Mc band it is less than 1.1.

III. CONCLUSIONS

For considerable number of waveguide lossless two-ports the frequency behavior of residual reflection coefficients may be approximated by circular arcs. Each two-port of such a kind has one fixed pair of optimum reflection coefficients (g_{rk} and g_{sk}), which are transformed through the two-port independent of frequency. To utilize this fact for wide-band matching of two-ports, the reflection coefficient of external input and output circuit must be made equal to g_{rk} and g_{sk} . In the method described, the matching is attained by putting the inductive obstacles at a certain distance from two-port terminals. The position and the value of inductive susceptances is calculated from measured curves of residual input and output reflection coefficients plotted on a Smith diagram.

For the sake of clarity, it is assumed that the susceptibility of obstacles does not vary with the frequency. This is not true for a very large band of frequencies, and the correction of position and value of obstacle must be calculated; this problem is not treated in this paper.

The method presented is valid for lossless two-ports but can probably be extended to lossy two-ports.